Acta Chemica Scandinavica, 1997: 51: 199–210
Printed in UK – all rights reserved

ACTA
CHEMICA SCANDINAVICA
ISSN 0904-213X

Review Article

Ab Initio Calculations of EPR Parameters with Strong Vibronic Interactions†

B. Engels

Institut für Physikalische und Theoretische Chemie, Universität Bonn, Wegelerstrasse 12, D-53115 Bonn, Germany

Engels, B., 1997. *Ab Initio* Calculations of EPR Parameters with Strong Vibronic Interactions. – Acta Chem. Scand. 51: 199–210. © Acta Chemica Scandinavica 1997.

In this paper some possibilities of *ab initio* treatments in the calculation of EPR parameters are discussed. After a brief introduction to the method we use to calculate the parameters, the influence of spin polarisation effects on differences between nitrogen compounds and their protonated radical cations will be shown. The second part of the review is devoted to dynamic effects. Using the electronic ground states of B_2H_2 and $B_2H_2^+$ as model cases the dependence of the parameters on vibronic quantum numbers is discussed in terms of the influence of the molecular geometry on the electronic parameters and the energy location and electronic character of the vibronic levels in questions. A brief introduction to the model we use to describe the influence of nuclear motion on magnetic hyperfine coupling constants is given.

Electron paramagnetic resonance (EPR) spectroscopy is a powerful tool that provides valuable information on spin distribution in free radicals. It is based on the magnetic hyperfine interaction which describes the interaction between the electron spin ($\vec{S}$) and the spins of the various nuclei ($\vec{I}_N$). The magnetic hyperfine interaction can be divided into an isotropic part, A_{iso}, which is proportional to the spin density at the given nucleus, and an anisotropic part, which describes the dipole–dipole interaction between $\vec{I}_N$ and $\vec{S}$ and has the form of a second-rank tensor.[1] Since the interaction occurs at each nucleus with a non-vanishing spin $\vec{I}_N$, a map of the spin distribution over the whole molecule can be obtained from EPR spectra.

In the present work possibilities of theoretical treatments in the calculation of EPR parameters is discussed. After a brief introduction to the MRD-CI/B_K method used for the calculation of electronic magnetic hyperfine coupling constants (hfcc) we will focus on spin polarisation effects found to be important for the interpretation of EPR spectra of nitrogen compounds and their protonated radical cations. Spin polarisation effects arising due to the interaction between the unpaired electron and electron pairs can easily be studied using theoretical methods.

In the second part we will concentrate on the influence of nuclear motions on hfcc, which is neglected in most theoretical studies. Neglect of this influence is justified in cases where A_{iso} depends linearly on the nuclear geometry *and* all vibrations are well described by a harmonic ansatz. In all other cases a reliable reproduction of A_{iso} can be achieved only by proper averaging over the nuclear motion. In the present work we discuss some recent results obtained for the B_2H_2 molecule and its cation $B_2H_2^+$.

Theory

The isotropic hyperfine coupling constant A_{iso} of a nuclear center is defined as[1] eqn. (1), where the term

$$A_{iso}(N) = \frac{8\pi}{3} g\beta_N \beta_e g_N \frac{1}{S} \left\langle \Psi \left| \sum_{k=1}^{n} \delta(r_k - r_N) s_z(k) \right| \Psi \right\rangle \quad (1)$$

in the brackets is the total spin density of the electrons at the location of the nucleus N. The term g is the g value for the electrons in the radical, while β_N is the Bohr magneton. In the present work g was set to the value for the free electron g_e. The quantities g_N and β_N are the nuclear g factor and the value for the nuclear magneton, respectively.

The wavefunction Ψ appearing in eqn. (1) represents, generally, the total molecular wavefunction. The hfcc

† Lecture held at the 14th International Conference on Radical Ions, Uppsala, Sweden, July 1–5, 1996.

obtained if Ψ is replaced by the electronic wavefunction, ψ, calculated in the framework of the Born–Oppenheimer approximation (neglect of nuclear motion) will be called 'electronic hfcc'. To include the effect of the nuclear motion Ψ must include the nuclear part, and subsequent integration over the vibrational coordinates must be performed. In the following, the values obtained by proper averaging over the nuclear motion will be abbreviated as 'vibronic hfcc'.

Before discussing effects arising due to the nuclear motion, let us first concentrate on reliable computations of electronic isotropic hfcc which is still a very difficult task for *ab initio* calculations.[2–6] In configuration interaction (CI) calculations, it is important to account for the effect of higher excitations with respect to the main configuration. In the multi-reference CI (MR-CI) approach, A_{iso} depends strongly on the number of reference configurations and, if configuration-selected MR-CI calculations are performed, the composition of the variationally handled MR-CI space is also crucial for the description of A_{iso}.

For a discussion of the effects found in CI calculations it is helpful to consider the influence of a configuration neglected in smaller calculations but taken into account in improved computations.[7] The added configuration changes the value of a property (calculated as an expectation value) for two reasons. The first influence arises because this configuration additionally appears in the CI expansion of the wavefunction (direct effect). A second effect arises because the added configuration interacts with configurations already included in the smaller calculation. Because of this interaction the coefficients of these configurations differ to some extent if one goes from the wavefunction obtained from the smaller calculation to the wavefunction computed in the larger (improved) calculation. Using the larger wavefunction to calculate a property, these changes will also influence the computed value of the property (indirect effect). In fact, we have been able to show[7] that for higher excitations (triples and quadruples) the second effect is far more important than the first one. For single and double excitations both effects have to be taken into account. A detailed study of both effects can be taken from Refs. 7–9.

The MRD-CI/B_K method[8–10] represents an efficient approach that includes all important effects. Direct effects are covered by individually selecting MR-CI calculations (usually including 25 000–30 000 configurations) using a large number of reference configurations. The reference configurations are selected according to two criteria. All configurations with squared coefficients larger than 0.001 in the final wavefunction should be included in the reference configuration set. Additionally, the importance of single excitations with respect to the main configurations are checked using a one-electron spin density matrix. These single excitations are also added to the reference configuration set. Important indirect effects of the neglected configurations are included via the B_K method.[11] Our new ansatz differs to some extent from older implementations which used small CI spaces to cover the direct contributions but included all configurations in the B_K treatment.[12,13] Our implementation starts from large CI spaces but does not include all configurations in the B_K part. In our approach all single excitations with respect to important reference configurations are included in the B_K correction. In addition those configurations having a coefficient larger than 0.03 are corrected via the B_K treatment. This approach is shown to be sufficiently sophisticated because the relaxation of coefficients of less important configurations was found to be less important.[8,9]

A remarkable example of the accuracy of the MRD-CI/B_K method is the C_α center of $C_\alpha C_\beta O$ given in Table 1.[14] The B_K correction improves the isotropic hfcc from -7.8 MHz (MRD-CI) to 30.7 MHz (MRD-CI/B_K). Due to this improvement $A_\perp$ increases from 17.9 to 56.3 MHz (exptl., 57 ± 3 MHz) while the value of $A_\parallel$ goes from -50.3 MHz to -20.7 MHz (exptl., -17 ± 3 MHz). It is seen that the CIS method, which is able to give very accurate isotropic hfcc for many systems, fails to predict the isotropic hfcc of the C_α center.

Influence of spin polarisation effects on the EPR structure of nitrogen compounds

Radicals possessing one or more nitrogen centers, both as radical cations and neutral radicals, have attracted growing attention in recent years. The radical compounds $(CH_3)_2N$ and $C_2H_6NH^+$ have been studied by Danen and coworkers[16,17] who corrected the results obtained by Hadly and Volman.[18] For both compounds, hfcc were

Table 1. Theoretical hyperfine coupling constants (in MHz) for CCO ($^3\Sigma_u^-$) using different theoretical treatments.

$C_\alpha C_\beta O$	C_α			C_β			O		
	A_{iso}	$A_\perp$	$A_\parallel$	A_{iso}	$A_\perp$	$A_\parallel$	A_{iso}	$A_\perp$	$A_\parallel$
CIS	17.3	43.7	−35.5	−33.8	−32.4	−36.6	−26.6	−43.3	6.8
CISD	−8.0	17.9	−59.7	−34.8	−32.0	−40.2	−5.2	−17.7	19.8
MRD-CI	−7.8	17.9	−59.3	−34.0	−31.7	−38.7	−12.7	−26.8	15.7
MRD-CI/B_K	30.7	56.3	−20.7	−30.7	−29.6	−32.9	−23.8	−41.3	11.2
Exptl.[a]	32(3)	57(3)	−17(3)	−30(3)	−26(3)	−32(3)			

[a] Ref. 15, the numbers in parentheses are the experimental errors, the signs of the experimental values were taken from the theoretical calculations.

interpreted by assuming that the nitrogen center is sp^2 hybridized and the unpaired electron occupies the nitrogen p-orbital perpendicular to the C–N–C plane. In their second paper Danen *et al.*[17] compared the radical $(CH_3)_2N$ with its protonated cation $(CH_3)_2NH^+$. While the higher isotropic hfcc of the β protons (27.36 G vs. 34.27 G) were attributed to hyperconjugation effects, the reason for the trend seen for $A_{iso}(^{14}N)$ (14.78 G to 19.28 G) could not be explained.

Four-membered rings containing one nitrogen atom, $C_3H_6N/C_3H_6NH^+$, have been studied by Qin and Williams[19] and Sjöqvist *et al.*[20,21] The studies show that the molecular structure of the radical cation seems to be planar, while the neutral radical has a puckered geometry. Furthermore it was concluded that both compounds possess an electronic structure similar to that of $(CH_3)_2N$ or $C_2H_6NH^+$. Again the isotropic hfcc of the neutral species were found to be much smaller than those of the protonated compounds.

The three membered rings, $C_2H_4N/C_2H_4NH^+$, have also been studied by Qin and Williams.[19] While the neutral species possesses the same electronic structure as C_3H_6N, the measured EPR spectrum of $C_3H_6NH^+$ pointed to a ring-opened structure, where the unpaired electron is located on the carbon centers.

Ab initio calculations were performed for $C_2H_6NH^+$[22] and the four-membered rings.[20,21] The computations confirmed conclusions regarding geometrical and electronic structures but the calculated isotropic hfcc turned out to be too inaccurate. For the nitrogen center deviations between experiment and theory were sometimes larger than 70%.

To resolve discrepancies between measured and calculated $A_{iso}(^{14}N)$ values we performed computations for all systems mentioned above ($C_3H_6N/C_3H_6NH^+$,[23] $C_2H_4N/C_2H_4NH^+$[24] and $C_2H_6N/C_2H_6NH^+$[25]). The geometries of the various compounds were optimised using the UMP2 method in combination with the 6–31G* AO basis set. The results were checked by QCISD calculations and some optimizations were performed using the DFT method (BLYP/6–31G*). The geometries obtained did not differ considerably from the previous results. The AO basis sets used to calculate the hyperfine coupling constants were selected according to Chipman.[26,27] Due to software limitations the size of the AO basis sets varied. The MRD-CI/B_K method was used in all calculations. Further details can be taken from the literature.[23–25]

Fig. 1 contains our results for $A_{iso}(^{14}N)$ together with the experimental data. It is obvious that we have managed to remove the large discrepancy between theory and experiment found for the nitrogen center in previous studies. A careful analysis of the C_3H_6N radical[23] revealed that both the AO basis set and computational methods were responsible for the failure of previous *ab initio* studies. Fig. 1 does not contain an experimental value for the ring structure of $C_2H_4NH^+$. Our results[24] confirm the interpretation of Williams and coworker[19]

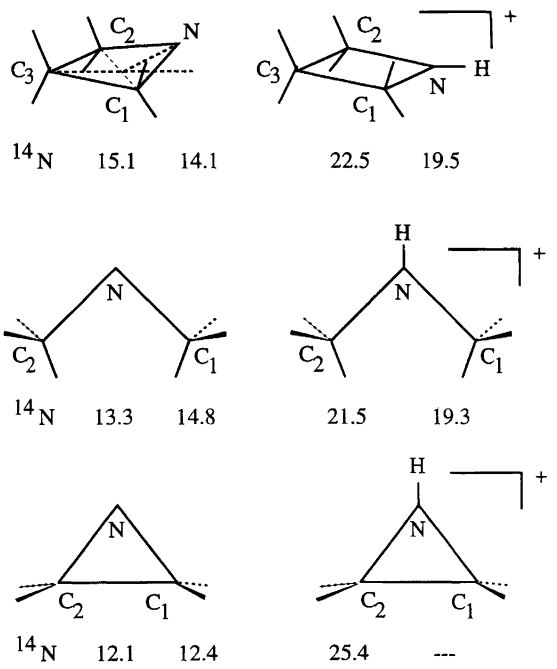

Fig. 1. Summary of $A_{iso}(^{14}N)$ for some nitrogen radicals and their protonated cations. The left-hand value gives the theoretical result while the right-hand number gives the experimental value of $A_{iso}(^{14}N)$.

who suggested that their EPR measurements point to a ring-opening process for $C_2H_4NH^+$.

Both experiment and theory find the isotropic hfcc of the protonated species to be 5–6 G larger than those of the neutral radical. In order to explain the differences between neutral and protonated species spin polarization effects were analyzed in detail. Due to its shape the SOMO [Fig. 2(a)], cannot contribute to $A_{iso}(^{14}N)$. In the following discussion C_2H_6N and $C_2H_6NH^+$ are used as model systems. Similar trends were found in all other examples. An estimate of the influence of a doubly occupied shell on the isotropic hfcc can be obtained by comparing the result of a core calculation in which the orbital under consideration is frozen (no excitations are allowed out of the given orbital) with the isotropic hfcc obtained from an all-electron calculation. The results are given in Table 2. As mentioned above the RHF value (first line) of $A_{iso}(^{14}N)$ is zero (no contribution from the SOMO). The second line shows the hfcc calculated with an all-electron CISD calculation, while the other hfcc are obtained by freezing the indicated orbital. The procedure can give only general trends since the interaction between doubly occupied shells is not properly accounted for. The largest difference in $A_{iso}(^{14}N)$ between the radical cation and the neutral radical is found when the $6a_1$ [Fig. 2(b,c)] or the $5a_1$ [Fig. 2(d,e)] orbital is frozen. For example $A_{iso}(^{14}N)$ of the cationic drops by 4 G if no excitations are allowed out of $6a_1$. The same procedure causes an increase of about 2 G for the neutral radical. When excitations out of $5a_1$ are not allowed $A_{iso}(^{14}N)$ decreases by about 12 G in the neutral species but only

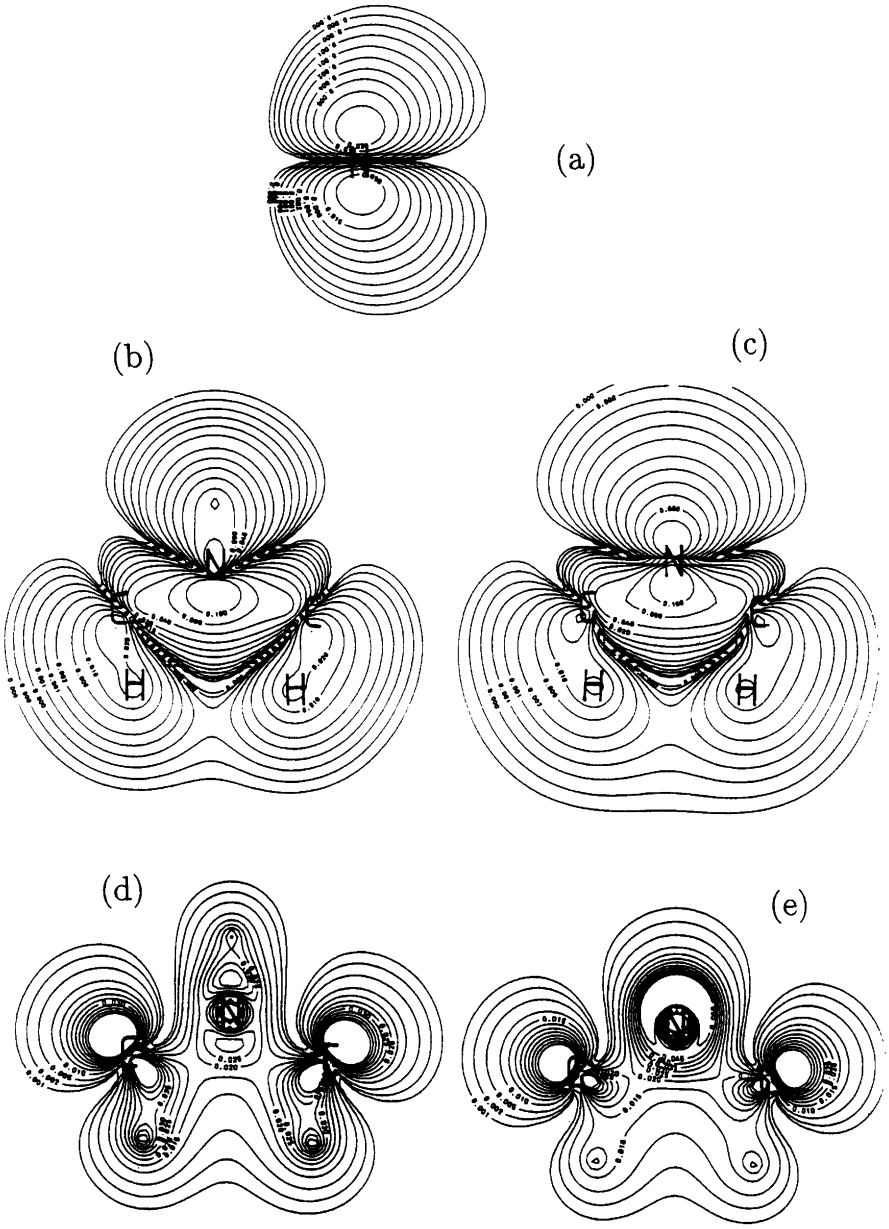

Fig. 2. Charge density contour plot of ground state X^2B_1 MOs of $(CH_3)_2N$ and $(CH_3)_2NH^+$: (a) singly occupied orbital (SOMO) $2b_1$ of $(CH_3)_2NH^+$ cut perpendicular to the CNC plane containing the nitrogen center; (b), (c) $6a_1$ orbital of $(CH_3)_2NH^+$ and $(CH_3)_2N$; (d), (e) $5a_1$ orbital of $(CH_3)_2NH^+$ and $(CH_3)_2N$; (b)–(e) give cuts through the CNC plane.

4 G in the protonated compound. The different behaviour of $A_{iso}(^{14}N)$ reflects the different nature of these orbitals in each molecule. The influence of all other orbitals on $A_{iso}(^{14}N)$ are almost the same in both compounds. It is worth noting that $1a_1$, which is the 1s orbital of the nitrogen center, also contributes strongly to $A_{iso}(^{14}N)$.

Influence of nuclear motion on magnetic hfcc. In most theoretical studies the influence of the nuclear motion on hfcc is neglected. This approach is justified in cases where A_{iso} depends linearly on the nuclear geometry *and* all vibrations are reliably described by a harmonic ansatz. An example is the $^3\Pi_u$ state of the C_2 molecule[28] where only a minor dependence of A_{iso} on the vibrational quantum number is found. In other cases a reliable reproduction of A_{iso} can be achieved only if proper averaging over the nuclear motion is performed. As has been shown in various studies,[29–38] the variation of the vibronically averaged hfcc from one vibronic level to another reflects generally three effects more or less connected with each other: (1) geometry dependence of the electronic hfcc; (2) the energy location of the vibronic level in question because the bending amplitude increases with increasing vibronic level energy and (3) the electronic character of the vibronic state if mixing between electronic states has to be taken into account. In the

Table 2. Summary of calculations performed to study spin polarization effects in C_2H_6N and $C_2H_6NH^+$. All values are given in Gauss.

	$C_2H_6NH^+$				C_2H_6N		
MO[a]	N	C	H_β	H_α	N	C	H_β
No correlation (RHF)							
	0.0	0.0	23.4	0.0	0.0	0.0	18.8
Correlation of all electrons (SD-CI)[b]							
	11.7	−10.0	35.9	−18.7	8.0	−11.5	28.8
Correlation of the valence shell							
$6a_1$	9.4	−10.2	36.6	−14.7	9.7	−10.8	29.4
$5a_1$	7.3	−11.0	35.3	−15.8	−4.3	−14.1	28.8
$4a_1$	−3.6	−13.3	36.8	−6.4	−2.9	−13.2	29.2
$3a_1$	6.0	−1.2	35.4	−17.6	3.4	−2.9	28.4
$1b_1$	13.4	−10.2	29.6	−20.3	9.3	−11.7	23.6
$4b_2$	13.3	−9.4	35.7	−20.4	9.6	−9.5	28.8
$3b_2$	13.4	−10.7	36.0	−19.0	9.4	−12.5	28.9
$2b_2$	13.0	−5.5	34.8	−19.6	9.1	−7.2	28.0
$1a_2$	13.4	−10.2	31.9	−20.1	9.3	−11.9	25.7
Correlation of the 1s shell							
$2a_1/1b_2$[c]	12.1	−9.9	36.0	−18.8	8.3	−11.7	28.9
$1a_1$[d]	31.8	−10.0	36.0	−18.8	27.1	−11.5	28.9

[a] No excitations out of the given MO were allowed (see the text). [b] Reference: SD-CI, all electrons correlated. [c] 1s shell of the carbon centers. [d] 1s shell of the nitrogen center.

present work the electronic ground state of the B_2H_2 molecule, $X^3\Sigma_g^-$, and the electronic ground state of its radical cation, $B_2H_2^+$ ($X^2\Pi_u$), will be used to discuss some interesting effects. In both systems the description of the *trans*- and *cis*-doubly degenerate bending modes is found to be sufficient to include the major influence arising from the nuclear motion. Mixing of electronic states can be neglected for the $X^3\Sigma_g^-$ state but must be taken into account to describe the influence of the nuclear motion in the $X^2\Pi_u$ state of $B_2H_2^+$ (Renner–Teller effect). After a very brief introduction to the model we use to describe the *trans* and *cis* doubly degenerate bending modes, including Renner–Teller effects, the results obtained for both systems will be discussed.

Calculation of vibronically averaged hfcc (including non-adiabatic effects)

The Renner–Teller effect is one of the best studied examples of the breakdown of the Born–Oppenheimer approximation. It can be considered as a consequence of two different electronic states coupled with one another through the electronic–rotational Coriolis interaction.[39] For the present examples it results from the existence and mutual coupling of two electronic states in the bent nuclear conformation, which correlate with the same degenerate (Π, Δ, ...) species at the linear molecular geometry. Experimentally the interaction is reflected in the complicated irregular vibrational structure of the electronic spectra and for molecular properties, e.g., magnetic hyperfine coupling constants, a strong dependence on the rovibrational quantum numbers is found. For many systems the effect can already be seen if the results obtained for the vibrational ground states of two different isotopomers are compared. For a review concerning this subject the reader is referred to Ref. 33.

The first theoretical model for handling the Renner–Teller effect in tetra-atomics was developed by Petelin and Kiselev.[40] They elaborated a perturbative approach and derived formulae that describe several special coupling cases, the majority of them concerning situations in which only one of the two bending modes was excited. In the present work we use the treatment of Perić *et al.*[41] who developed a variational approach for an *ab initio* treatment of the Renner–Teller effect in tetra-atomic molecules, generalizing the original model of Petelin and Kiselev. In the present work only a brief introduction to this approach will be given. More details can be taken from Refs. 36 and 37.

The (spinless) model Hamiltonian describing the *trans* and *cis* doubly degenerate bending modes of a symmetric tetra-atomic molecule (A–B–B–A) with a linear equilibrium geometry is expressed in terms of the symmetry coordinates (π_u, π_g) of the $D_{\infty h}$ point group, eqn. (2).

$$H = -\frac{1}{2\mu_T}\left(\frac{\partial^2}{\partial\rho_T^2} + \frac{1}{\rho_T}\frac{\partial}{\partial\rho_T} + \frac{1}{\rho_T^2}\frac{\partial^2}{\partial\phi_T^2}\right) - \frac{1}{2\mu_c}\left(\frac{\partial^2}{\partial\rho_c^2} + \frac{1}{\rho_c}\frac{\partial}{\partial\rho_c} + \frac{1}{\rho_c^2}\frac{\partial^2}{\partial\phi_c^2}\right) + V_T^{\pm}(\rho_T) + V_C^{\pm(\rho_C)} \quad (2)$$

ρ_T represents the (small amplitude) displacements of the terminal nuclei perpendicular to the *a*-axes and ϕ_T the azimuthal angle of the instantaneous molecular plane for the π_g(*trans*)-type bending. The corresponding *cis* coordinates are ρ_c and ϕ_c. The expressions $\mu_T = 2mMR^2/[MR^2+m(R+2r)^2]$ and $\mu_C = 2mMr^2/(m+M)$ are the reduced masses for infinitesimal *trans*- and *cis*-bending, respectively; in our case, $m = M_H$, $M = M_B$, r = B–H, R = B–B. $V_T^{\pm}(\rho_T)$ represents the potential energy curves for the *trans* bending vibrations and $V_C^{\pm}(\rho_C)$ their *cis* bending counterparts. The superscripts + and − denote the electronic states at which wavefunctions are either invariant or change sign upon reflection in the molecular plane, respectively. It is assumed that the potential energy part of the Hamiltonian does not involve cross terms coupling *trans* and *cis* bending vibrations. Azimuthal coordinates ϕ_T and ϕ_C can conveniently be replaced by their linear combinations,[40] eqn. (3). The so

$$\phi = 1/2(\phi_T + \Phi_C) \qquad \gamma = 1/2(\phi_T - \Phi_C) \quad (3)$$

defined coordinate ϕ is conjugate to the *a*-component of the total vibrational angular momentum of the molecule.

As a basis for the representation of the Hamiltonian (2), we employ functions of the form eqn. (4), where θ

$$e^{i\Lambda\theta}e^{il_T\phi_T}\,e^{il_C\phi_C}R_{v_T,l_T}(\rho_T)R_{v_C,l_C}(\rho_C)$$
$$=e^{iK\phi}e^{i\Lambda(\theta-\phi)}e^{il\gamma}R_{v_T,K-\Lambda+l/2}(\rho_T)R_{v_C,K-\Lambda-l/2}(\rho_C)$$
$$e^{i\Lambda\theta}e^{il_T'\phi_T}e^{il_C'\phi_C}R_{v_T',l_T'}(\rho_T)R_{v_C',l_C'}(\rho_C)$$
$$=e^{iK\phi}e^{-i\Lambda(\theta-\phi)}e^{im\gamma}R_{v_T',K+\Lambda+m/2}(\rho_T)R_{v_C',K+\Lambda-m/2}(\rho_C) \quad (4)$$

denotes the coordinate conjugated to the a-component of the electronic angular momentum and Λ is the absolute value of the corresponding quantum number ($\Lambda=1$ for electronic Π and $\Lambda=0$ for electronic Σ states). l_T and l_C as well as l_T' and l_C' are signed quantum numbers corresponding to the operators $l_a{}^T=-i\partial/\partial\phi_T$ and $l_a{}^C=-i\partial/\partial\phi_C$, respectively. l and m are defined by $l=l_T-l_C$, $m=l_T'-l_C'$. K is the quantum number of the total angular momentum N_z (excluding spin) along the a-axis, and is given by eqn. (5) Since the model Hamiltonian

$$K=\Lambda+l_T+l_C \qquad K=-\Lambda+l_T'+l_C' \quad (5)$$

we use commutes with N_z, the quantum number K is conserved and the vibronic problem can be solved for each K value separately. Because the degeneracy of the vibronic levels differing only in the sign of K is not lifted in the present approach only $+K$ values are calculated. $R_{v,l}$ represent the solutions of the radial equation of a two-dimensional harmonic oscillator with $l=v,v-2$, $v-4$, ..., 0 or 1. After integration over the angular coordinates the matrix elements diagonal with respect to the electronic basis functions obtain the form of eqns. (6) and (7), and the off-diagonal elements are eqns. (8) and (9).

$$\left\langle R_{v_T{}^i,l_T{}^i}\left|\frac{1}{2}(V_T{}^+ + V_T{}^-)-\frac{1}{2\mu_T}\left(\frac{\partial^2}{\partial\rho_T{}^2}+\frac{1}{\rho_T}\frac{\partial}{\partial\rho_T}+\frac{l_T{}^2}{\rho_T{}^2}\right)\right|\right.$$
$$\left.\times R_{v_T{}^j,l_T{}^j}\right\rangle \delta_{l_T{}^i,l_T{}^j}\delta_{l_C{}^i,l_C{}^j}\delta_{v_C{}^i,l_C{}^i} \quad (6)$$

$$+\left\langle R_{v_C{}^i,l_C{}^i}\left|\frac{1}{2}(V_C{}^+ + V_C{}^-)-\frac{1}{2\mu_C}\left(\frac{\partial^2}{\partial\rho_C{}^2}+\frac{1}{\rho_C}\frac{\partial}{\partial\rho_C}+\frac{l_C{}^2}{\rho_C{}^2}\right)\right|\right.$$
$$\left.\times R_{v_C{}^j,l_C{}^j}\right\rangle \delta_{l_T{}^i,l_T{}^j}\delta_{l_C{}^i,l_C{}^j}\delta_{v_T{}^i,l_T{}^i} \quad (7)$$

$$\left\langle R_{v_T{}^i,l_T{}^i}\left|\frac{1}{2}(V_T{}^+ - V_T{}^-)\right|R_{v_T{}^j,l_T{}^j}\right\rangle \delta_{l_T{}^il_T{}^j\pm2\Lambda}\,\delta_{l_C{}^il_C{}^j}\delta_{v_C{}^i,l_C{}^i} \quad (8)$$

$$\left\langle R_{v_C{}^i,l_C{}^i}\left|\frac{1}{2}(V_C{}^+ - V_C{}^-)\right|R_{v_C{}^j,l_C{}^j}\right\rangle \delta_{l_T{}^il_T{}^j}\,\delta_{l_C{}^il_C{}^j\pm2\Lambda}\,\delta_{v_T{}^i,l_T{}^i} \quad (9)$$

Because the $X^3\Sigma_g{}^-$ state is non-degenerate* (no splitting into V^+ and V^- upon bending) the off-diagonal matrix elements vanish and the diagonal part reduces to two non-interacting two-dimensional harmonic oscillators. As a consequence no Renner–Teller effect is observed. In this case ($\Lambda=0$) a K quantum number is constructed from only one combination of l_T and l_C. For a more detailed discussion see Refs. 36 and 41.

The model discussed above has two critical conditions. Because only the bending modes are explicitly taken into account in the kinetic energy part of the Hamiltonian [eqn. (2)], the bending motions should have insignificant coupling to the stretching modes. Secondly, the barrier of the torsion motion has to be low because this motion is described as a free rotation. Both conditions are normally fulfilled for small bending vibrations of linear molecules.[33,41] To describe the dependence of magnetic hfcc on rovibronic quantum numbers the potential energy surfaces describing the nuclear motions ($V_T{}^\pm$, $V_C{}^\pm$) and the corresponding electronic wavefunctions of the electronic states under consideration are needed. Additionally, the magnetic hyperfine coupling constants (as a function of the various molecular geometries) has to be computed. If stretching modes are also important for the description of a molecular property (which is not the case for the present systems) their influence can be included in the framework of the model in which the couplings between the various modes are neglected. Such a procedure turned out to be important for the description of BH_2.[32]

Ab initio investigation of vibrational effects on magnetic hyperfine coupling constants of $B_2H_2(X^3\Sigma_g{}^-)$

The thermal decomposition of binary boron species is potentially important in the creation of thin metallic films involved in the manufacture of semiconductor devices. Very recently, in an excellent study Knight and coworkers[42] described an experimental characterization of the ground state $X^3\Sigma_g{}^-$ of B_2H_2 using EPR techniques in neon and argon matrices at 4 K. For $A_{iso}(^{11}B)$ a value of -5.2 MHz was obtained, while -38.9 MHz was measured for $A_{iso}(H)$. However, *ab initio* calculations carried out in the framework of this study were not able to reproduce the experimental value for boron [-19.1 MHz vs. $-5.2(4)$ MHz], while quite good agreement was found for the hydrogen center [-36.5 MHz vs. $-38.9(5)$ MHz]. The negative values obtained for all isotropic hfcc result from spin polarisation effects. Contributions from the SOMO (π_u orbital) vanish. The electronic configuration of the $X^3\Sigma_g{}^-$ state in a linear nuclear arrangement is $1\sigma_g^2 1\sigma_u^2 2\sigma_g^2 3\sigma_g^2 1\pi_u^2$. In order to understand the descrepancies between theory and experiment we performed calculations using the MRD-CI/B_K method in combination with the AO basis set given by Chipman.[26] At the equilibrium geometry (linear arrangement with B–H = 2.231 bohr; B–B = 2.869 bohr) we obtained $A_{iso}(^{11}B)=-14.0$ MHz and $A_{iso}(H)=41.4$ MHz. Both values are somewhat different from the theoretical values obtained by Knight and coworker. The deviations could be ascribed to the improved theoretical treatment employed in the present work but this cannot

* We consider only spatial degeneracies.

explain the differences from the experimental value of $A_{iso}(^{11}B)$.

The large deviations between our values and the experimental ones point to a large influence of the nuclear motion. This expectation is based on the changes that occur in the electronic structure during the bending vibrations. Upon bending the axial symmetry is lowered to C_{2h} (*trans*-bending) or C_{2v} (*cis*-bending). In the *trans*-bending distortion of the molecule the electronic configuration is transformed into a $^3B_1$ state ($1a_1^2 1b_2^2 2a_1^2 2b_2^2 3a_1^2 1b_1^1 4a_1^1$) while a ^3B_g state ($1a_g^2 1b_u^2 2a_g^2 2b_u^2 3a_g^2 3b_u^1 1a_g^1$) is obtained by a *cis*-type distortion of B_2H_2. For both, an increase in the isotropic hfcc can be expected because the a_1 and the b_u orbital change their character from a pure π-orbital to a partial σ-type orbital. As a result a large influence of the nuclear motion on the computed isotropic hfcc is obtained as has been shown in many other systems.[33]

For the description of the vibrational effects we used the potential energy surface obtained in a current study[43] and calculated the magnetic hfcc as a function of the bending angles ρ_T and ρ_C. For the calculation of the potential energy surface (for more details see Ref. 43) including the symmetric B–H stretching, the B–B stretching, *trans*- and *cis*-bending as well as the torsional motion of the B–H groups with respect to one another, we used the standard MRD-CI method.[44,45] The atomic orbital (AO) basis employed in the calculations consists of a (9s5p) basis of Dunning in the [5s3p] contraction[46] augmented by a single Cartesian d function ($\alpha = 0.388$). For the hydrogen atoms the (8s2p)→[5s,2p] basis of Lie and Clementi[47] is employed. Additional Rydberg functions ($\alpha_{3s} = 0.019, \alpha_{4s} = 0.0047, \alpha_{3p} = 0.015, \alpha_{3d} = 0.015$) are centered in the midpoint of the B–B bond. In all calculations a core corresponding to the 1s orbitals of the boron atoms is kept doubly occupied. As shown in Ref. 36, both critical conditions for the applicability of our model used to describe the Renner–Teller effects are fulfilled. The relative rotations of the B–H groups around the B–B axis (torsion) are practically free (at least for a small variation from linearity considered in the present work) and, as expected from symmetry considerations, insignificant coupling of the bending modes to the stretch modes is found.

The quality of the atomic orbital (AO) basis set used in the calculation of the energy hypersurface is not expected to be high enough for the computation of accurate hfcc, particularly of the isotropic part of the hf tensor (see, for example Ref. 33). Thus in the present study we use the (10s6p2d/6s1p)→[6s3p2d/4s1p] AO basis set given by Chipman,[4] which is optimized for the calculation of hfcc. The electronic hfcc are calculated using the MRD-CI/B_K method[8] described above. In all calculations of the electronic hfcc as a function of the bending angles the bond distances are kept fixed at the values of B–H = 2.23 bohr and B–B = 2.869 bohr.

The calculated isotropic hfcc are given in Fig. 3. While $A_{iso}(^{11}B)$ strongly increases as a function of ρ_T, a much

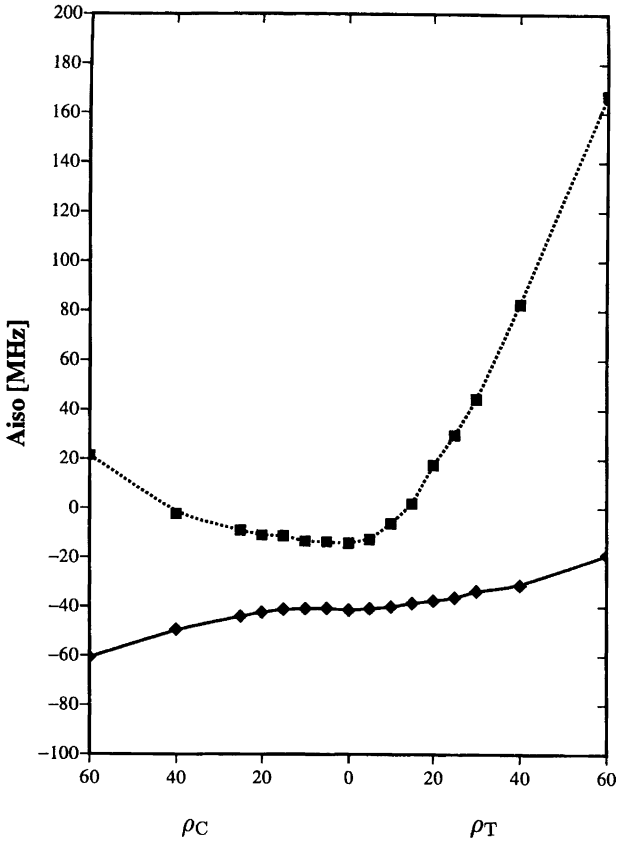

Fig. 3. Dependence of the electronic isotropic hfcc for the boron center (dotted line) and the hydrogen center (full line) for the $X e^3\Sigma_g^-$ state of B_2H_2 on the *trans* (right-hand side) and *cis* bending (left-hand side) coordinates ρ_T and ρ_C, respectively (see the text). The bond distances are kept fixed at the values of B–H = 2.231 bohr and B–B = 2.869 bohr.

smaller dependence is found with respect to ρ_C. Furthermore, $A_{iso}(H)$ shows only small changes. This behaviour can be explained by distortions of the SOMO upon bending. The shape of the SOMO for a *cis*-distorted nuclear arrangement (a_1-orbital) is displayed in Fig. 4(a), while Fig. 4(b) contains the information for the *trans*-distorted geometry (b_u orbital). The SOMO for the linear nuclear arrangement represents a π_u-orbital. The out-of-plane components of the π_u orbital are of less interest because they cannot directly contribute to A_{iso}. Deformation of the SOMO upon bending is seen for both *trans*- and *cis*-bending distortions. However, if the molecule is bent the SOMO [a_1 orbital depicted in Fig. 4(a)] changes in such a way that its nodal plane still contains the atomic centers. As a consequence its contributions to A_{iso} remain small for all *cis*-distortions, explaining the small influence of ρ_C an $A_{iso}(^{11}B)$ and $A_{iso}(H)$. The nodal plane of the b_u orbital (SOMO orbital of the trans-bent geometries) does not coincide with the boron centers. As a result the contributions from the b_u orbital to A_{iso}, which are zero for $\rho_T = 0$, will strongly increase for values of $\rho_T \neq 0$. This behaviour was found in many other systems.[33] $A_{iso}(H)$ increases to

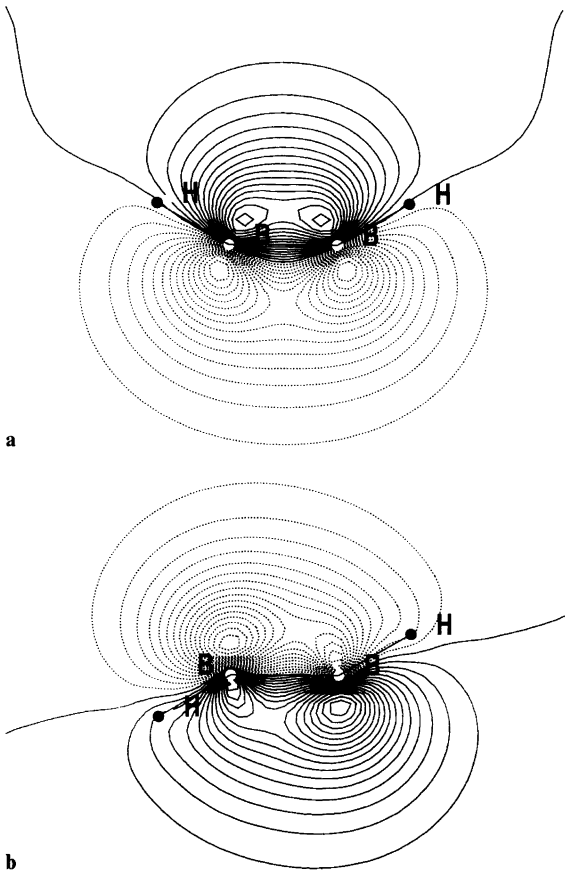

Fig. 4. Variation of the shape of the SOMO during the bending vibration: (a) *cis* bending of B_2H_2; (b) *trans* bending of B_2H_2. The positions of the boron centers are indicated by white spots.

a much smaller extent because the SOMO is concentrated at the boron centers. More details will be discussed in the context of the $B_2H_2^+$ cation (see below).

For the description of the vibrational effects the potential curve for the ^3B_g state (*trans* bending) is fitted by a polynomial of the 8th order (because this curve was found to be fairly anharmonic) and that for the $^3B_1$ state (*cis* bending) by a fourth-order polynomial in ρ_T and ρ_C, respectively. Employing as the basis the eigenfunctions of the corresponding four-dimensional harmonic oscillator, the vibrational energy levels and wavefunctions for each mode were computed variationally. The calculated frequencies (see Table 2) of the trans (Π_g) and cis (Π_u) bending modes are 597 cm^{-1} and 623 cm^{-1}, respectively.† This result is in fair agreement with theoretical values given by Tague and Andrews (549 cm^{-1} and 640 cm^{-1}), which used second-order Møller–Plesset perturbation theory and did not include anharmonic effects.[48] The hfcc functions displayed in Fig. 4 are fitted to the polynomials in ρ_T^{2n}, ρ_C^{2n} without cross-terms, and the vibronic mean values were computed as described in detail elsewhere.[33]

† The energy values represent the energy difference between the energy at the minimum of the potential energy surface and the vibrational level, divided by two.

The results are given in Table 3, which contains the mean values of $A_{iso}(^{11}B)$ and $A_{iso}(H)$ for the lower vibrational states. It can be seen that for $A_{iso}(^{11}B)$ the inclusion of vibrational effects is already essential for the vibrational ground state. The isotropic hfcc of the boron centers calculated for the lowest vibrational state [$A_{iso}(^{11}B) = -5.2$ MHz] differs considerably from the electronic value obtained at the equilibrium geometry [$A_{iso}(^{11}B) = -14.0$ MHz] and agrees excellently with the experimental value [$A_{iso}(^{11}B) = -5.2$ MHz) given by Knight and coworkers.[42] As expected, the main effect arises due to the *trans* bending mode (90%) while the *cis* bending mode is less important. This is underlined by the strong dependence of $A_{iso}(^{11}B)$ on the vibrational quantum numbers v_T and l_T. For $A_{iso}(H)$ the effect is much smaller, but the vibrational averaging shifts the calculated value towards the experimental value.

Ab initio investigation of vibrational effects on magnetic hyperfine coupling constants of $B_2H_2^+$ ($X^2\Pi_u$)

The electronic configuration of the $X^2\Pi_u$ state of $B_2H_2^+$ is obtained from the configuration of the $X^3\Sigma_g^-$ state of B_2H_2 by taking one electron out of the π_u orbital. For the linear nuclear arrangement ($D_{\infty h}$ point group) one obtains $1\sigma_g^2 1\sigma_u^2 2\sigma_g^2 3\sigma_g^2 1\pi_u^1$. Upon bending, the $X^2\Pi_u$ splits into two non-degenerate electronic states. At the *trans*-bending the states $^2B_1: 1a_1^2 1b_2^2 2a_1^2 2b_2^2 3a_1^2 1b_1^1$ and $^2A_1: 1a_1^2 1b_2^2 2a_1^2 2b_2^2 3a_1^2 4a_1^1$ arise, while at the *cis*-bending the states $^2B_u: 1a_g^2 1b_u^2 2a_g^2 2b_u^2 3a_g^2 3b_u^1$ and $^2A_u: 1a_g^2 1b_u^2 2a_g^2 2b_u^2 3a_g^2 1a_g^1$ are obtained.

For the calculation of the potential energy surfaces and the magnetic hfcc, the same methods as described in the context of the B_2H_2 molecule were used. The equilibrium bond distances calculated (B–H = 2.22 bohr, B–B = 3.05 bohr) are in a very reasonable agreement with prior results of Curtis and Pople (2.215 and 3.025 bohr).[49] As shown in Ref. 36, both critical conditions for the applicability of our model for describing the nuclear motion are fullfilled. Fig. 5 displays the *trans*- and *cis*-bending potential curves used for the description of the Renner–Teller effect. In these calculations the bond lengths were kept fixed at their equilibrium bond distances (B–H = 2.22 bohr, B–B = 3.05 bohr).

For the linear nuclear arrangement the values $A_{iso}(^{11}B) = 1.3$ MHz and $A_{iso}(H) = -47.9$ MHz were computed. These values are determined only by spin-polarisation effects (indirect contributions) because the SOMO represents a π_u orbital at the linear nuclear arrangement. Compared with the ground state $X^3\Sigma_g^-$ of the neutral B_2H_2 [$A_{iso}(^{11}B) = -14.0$ MHz, $A_{iso}(H) = -41.4$ MHz see above], $A_{iso}(^{11}B)$ is shifted by about 15 MHz while a shift of -6 MHz is found for $A_{iso}(H)$, reflecting changes in spin polarisation effects due to the additional unpaired electron in B_2H_2. The different sign in the shifts of $A_{iso}(^{11}B)$ and $A_{iso}(H)$ results from the

Table 3. Energy levels and vibronic mean values of the isotropic hfcc for boron and hydrogen atoms in the $X^3\Sigma_g^-$ state of $H^{11}B^{11}BH$.

Present work							Exptl.[42]	
Π_u		Π_g						
v_C	l_C	v_T	l_T	E/cm^{-1} [a]	$A_{iso}(^{11}B)$/MHz	$A_{iso}(H)$/MHz	$A_{iso}(^{11}B)$/MHz	$A_{iso}(H)$/MHz
0	0	0	0	0	−5.2	−39.2	−5.2(4)	−38.9(5)
0	0	1	1	599	17.0	−38.3	—	—
1	1	0	0	623	−4.4	−39.2	—	—
Linear geometry					−14.0	−41.4		

[a] Obtained as $E_{v_T, l_T, v_C, l_C} - E_{v_T=l_T=v_C=l_C=0}$.

fact that spin polarisation effects arising from the valence shell are positive for heavier atoms but negative for hydrogens. The values of both compounds are much smaller than those found in the BH_2 molecule [$A_{iso}(^{11}B) = 60$ MHz, $A_{iso}(H) = -75$ MHz].

The dependence of $A_{iso}(^{11}B)$ on the bending angles ρ_T and ρ_C is given in Fig. 6. An increase in $A_{iso}(^{11}B)$ is found for the ^2B_u and the $^2A_1$ component while only minor changes in $A_{iso}(^{11}B)$ are computed for the ^2A_u and $^2B_1$ states. The small change of A_{iso} for the latter is the result of the SOMOs being perpendicular to the molecular plane of the bent molecule. For the ^2B_u and the $^2A_1$ components (b_u^1 and a_1^1 occupation, respectively), the

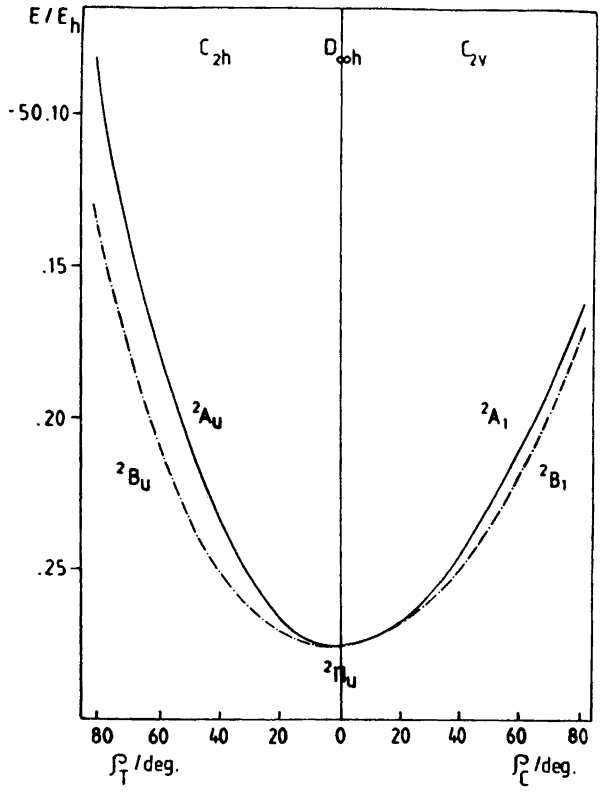

Fig. 5. trans and *cis* bending potential curves for the components of the $X^2\Pi_u$ state of $B_2H_2^+$ calculated with the B–H bond length kept fixed at 2.196 bohr and a B–B distance of 2.90 bohr.

SOMOs lie within the molecular plane which explains the strong increase in $A_{iso}(^{11}B)$. The reasons for the difference between the *trans*- and *cis*-bending are the same as those found in B_2H_2. The stronger increase found for $B_2H_2^+$ results from the more compact form of the molecular orbitals due to the positive charge.

For the dependence of $A_{iso}(H)$ on ρ_T and ρ_C, equivalent behaviour as calculated for the boron centers exists (Fig 7). For example, a considerable variation of $A_{iso}(H)$ is found only within the ^2B_u and $^2A_1$ states while for ^2A_u and $^2B_1$, where the direct contribution is zero due to the shape of the SOMO, again nearly no dependence on ρ_T and ρ_C is obtained. As with the neutral B_2H_2 molecule, the variations in $A_{iso}(H)$ are much smaller than the changes found for $A_{iso}(^{11}B)$. However, contrary to $A_{iso}(^{11}B)$ the sign of the variations in $A_{iso}(H)$ found for the ^2B_u and $^2A_1$ states are opposite, pointing to the fact that spin polarisation effects are important for the description of $A_{iso}(H)$, while direct contributions from the SOMO are smaller. As an example, the increase of $A_{iso}(H)$ found for the ^2B_u state (≈ 30 MHz) results from a decrease in the indirect contributions (−48 MHz to −30 MHz) while variations in the direct contribution are smaller (8 MHz). For the $^2A_1$ state $A_{iso}(H)$ decreases by about 40 MHz [$A_{iso}(\rho_C=0) = -48$ MHz, $A_{iso}(\rho_C=60) = -86$ MHz]. As already discussed for the ^2B_u state the variations result from changes in spin polarisation effects (indirect contributions), which changes from −48 MHz to −85 MHz. Because the increase of the direct contribution is very small (≤ 1 MHz) for the $^2A_1$ state an overall decrease of $A_{iso}(H)$ is found. As already discussed for the linear nuclear arrangement spin polarisation effects [on $A_{iso}(H)$ and $A_{iso}(^{11}B)$] seem to be larger in the radical cation $B_2H_2^+$ (π_u^1 occupation) than in its neutral counterpart B_2H_2 (π_u^2 occupation). The increase in the spin polarisation effects may result from the positive charge of $B_2H_2^+$.

The results of our computations of vibronically averaged values for the isotropic hfcc of hydrogen and boron in the lowest vibronic levels (0–1000 cm^{-1} with respect to the lowest level) of $^{11}B_2H_2$ are presented in Table 4. The vibronic states are labelled by the quantum numbers of the dominating basis functions. In addition we give

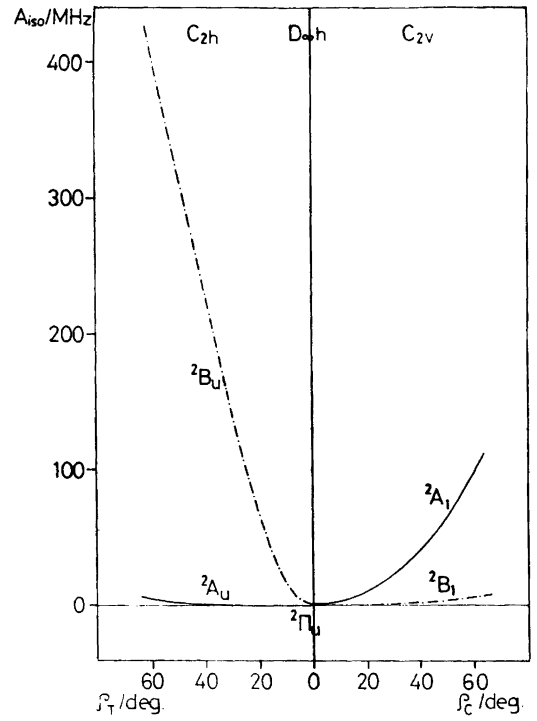

Fig. 6. Dependence of the electronic isotropic hfcc for the boron centers [$A_{iso}(^{11}B)$] in the electronic states of $B_2H_2^+$ correlating with $X^2\Pi_u$ on the *trans* (left-hand side) and *cis* bending (right-hand side) coordinates ρ_T and ρ_C, respectively. The bond lengths are kept fixed at B–H = 2.22 bohr and B–B = 3.05 bohr.

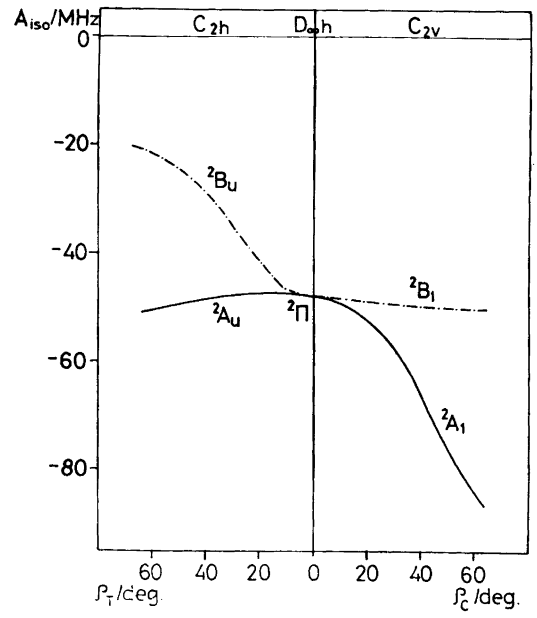

Fig. 7. Dependence of the electronic isotropic hfcc for the hydrogen centers [A_{iso}(H)] on the *trans* and *cis* bending coordinate (see also Fig. 6).

quantities called ^2B_u, ^2A_u, $^2B_1$ and $^2A_1$ state character. They represent the sums of squared expansion coefficients corresponding to the respective electronic basis functions. For convenience the sum of the characters for each particular vibronic state is chosen to be one and for each bending coordinate (*trans* or *cis* bending) it is 0.5.

As found for the neutral B_2H_2 molecule the general characteristic of the computed vibronic mean values is a relatively small dispersion of the results for the hydrogen centers and very erratic distribution of the vibronic mean values for $A_{iso}(^{11}B)$. The apparently erratic distribution of the values for the vibronic hfcc of the boron atom (shown in Table 4) can easily be explained in terms discussed at the beginning of this section, e.g., (1) geometry dependence of the electronic hfcc; (2) the energy location of the vibronic level in question because the bending amplitude increases with increasing vibronic level energy and (3) the electronic character of the vibronic state. An analysis of Table 1 shows that the varying contribution from ^2B_u is the main reason for the erratic distribution of the vibronically averaged $A_{iso}(^{11}B)$.

We have already shown how vibronic averaging affects numerical values for the hfcc; moreover the results of the present *ab initio* computations give clear insight into the mechanisms determining the values of hfcc in particular vibronic states. However, it is interesting to take another point of view and try to find the answer for the question: how can information about the vibronic coupling from the experimentally observed magnetic hyperfine structure of the spectrum be obtained? One possibility is a comparison of the results for various isotopomers of the same molecule. To check this point for the present case we calculated the vibronic energy levels and the isotropic hfcc of $B_2D_2^+$ for the $X^2\Pi_u$ state. The results obtained for the three lowest states are given in Table 5. If the nuclear motions were ignored both $B_2H_2^+$ and $B_2D_2^+$ would possess equal values for $A_{iso}(^{11}B)$. Our calculations in which the nuclear motion is taken into account show that already for the lowest vibronic level the value of $A_{iso}(^{11}B)$ for $B_2D_2^+$ is roughly 20% ($\approx$2MHz) lower than for $B_2H_2^+$. This unusual effect is a consequence of the fact that the vibronic levels of $B_2D_2^+$ lie closer to the minimum of the potential surface than do their $B_2H_2^+$ counterparts. Thus in the lowest vibronic state of $B_2D_2^+$, the turning point of the classical bending vibration corresponds to a smaller deviation from linearity than in $B_2H_2^+$. Because the magnitude of the electronic hfcc increases with increasing deviation from linearity, the vibronic $A_{iso}(^{11}B)$ in $B_2D_2^+$ is smaller than in $B_2H_2^+$. Note that in the above example the effects arising from the electronic composition of the vibronic states in question are small because the character of the lowest vibronic level is very similar in both isotopomers. In other vibronic levels the effects listed above are expected to contribute significantly to the vibronic values of hfcc.

Summary

In the present work we discuss some possibilities of theoretical treatments in the calculation of EPR para-

Table 4. Vibronic energy levels and vibronic mean values of the isotropic hfcc for hydrogen and boron atoms in the $X^2\Pi_u$ state of $^{11}B_2H_2^+$. For an explanation see the text.

			State character				$\langle A_{iso}\rangle$/MHz	
E/cm^{-1} [a]	$(l_T\, v_T\, l_C\, v_C)$	Symmetry	^2B_u	^2A_u	$^2B_1$	$^2A_1$	H	^{11}B
0	(0000)	Π_u	0.2928	0.2072	0.2604	0.2396	−47.2	12.6
473	(−1100)(1100)	Π_u	0.4999	0.0001	0.2588	0.2412	−44.9	37.6
537	(00−11)(0011)	Π_g	0.2914	0.2086	0.4967	0.0033	−47.0	12.0
584	(0011)	Π_g	0.2928	0.2071	0.2707	0.2293	−47.6	13.3
634	(00−11)(0011)	Π_g	0.2944	0.2056	0.0040	0.4960	−48.3	14.9
665	(1100)	Π_u	0.3316	0.1684	0.2603	0.2397	−45.9	26.1
936	(−1100)(1100)	Π_u	0.0004	0.4996	0.2632	0.2368	−48.2	1.5

[a] E is given with respect to the lowest vibronic state.

Table 5. Vibronic energy levels and vibronic mean values of the isotropic hfcc for hydrogen and boron atoms in the $X^2\Pi_u$ state of $^{11}B_2D_2^+$. For an explanation see the text.

			State character				$\langle A_{iso}\rangle$/MHz	
E/cm^{-1} [a]	$(l_T\, v_T\, l_C\, v_C)$	Symmetry	^2B_u	^2A_u	$^2B_1$	$^2A_1$	D	^{11}B
0	(0000)	Π_u	0.2933	0.2067	0.2604	0.2396	−7.3	10.5
386	(−1100)(1100)	Π_u	0.4999	0.0001	0.2587	0.2413	−7.0	31.6
396	(00−11)(0011)	Π_g	0.2920	0.2080	0.4967	0.0033	−7.2	10.1

[a] E is given with respect to the lowest vibronic state.

meters. In the first part of the paper the influence of spin polarisation effects on the differences between the magnetic hyperfine coupling constants of nitrogen compounds and their protonated cations are studied. The second part of this review is devoted to the influence of nuclear motion on EPR parameters which is neglected in most theoretical studies. Various effects are discussed using the electronic ground states of B_2H_2 ($X^3\Sigma_g^-$) and $B_2H_2^+$ ($X^2\Pi_u$) as model cases. It is found that for such systems the vibronic interaction is already important for the description of the EPR parameters of the vibronic ground state. Vibronic effects can already be seen if the results for various isotopomers of the same molecule are compared.

Acknowledgements. This work was supported in part by the *Deutsche Forschungsgemeinschaft (DFG)* and the *Deutscher Akademischer Austauschdienst (DAAD)*. The author would like to thank all his colleagues who took part in the work presented in this review especially Professors M. Perić and S. D. Peyerimhoff. Special thanks go to Hans Ulrich Suter and Ming-Bao Huang.

References

1. McWeeny, R. *J. Chem. Phys. 42* (1965) 1717.
2. Feller, D. and Davidson, E. R. *Theor. Chim. Acta 68* (1985) 57.
3. Engels, B., Peyerimhoff, S. P. and Davidson, E. R. *Mol. Phys. 62* (1987) 109.
4. Chipman, D. M. *Theor. Chim. Acta 76* (1989) 73.
5. Feller, D. and Davidson, E. R. *Molecular Spectroscopy, Electronic Structure, and Intramolecular Interactions*, Springer-Verlag, New York 1991, p. 429.
6. Chipman, D. M. *Theor. Chim. Acta 82* (1992) 93.
7. Engels, B. *Theor. Chim. Acta 86* (1993) 429.
8. Engels, B. *Chem. Phys. Lett. 179* (1991) 398.
9. Engels, B. *J. Chem. Phys. 100* (1994) 1380.
10. Suter, H. U. and Engels, B. *J. Chem. Phys. 100* (1994) 2936.
11. Gershgorn, Z., Shavitt, I. and Intern. *J. Quantum Chem. 2* (1968) 751.
12. Rawlings, D. C. and Davidson, E. R. *Chem. Phys. Lett. 98* (1983) 424.
13. Segal, G. A. and Wolf, K. *Chem. Phys. 56* (1981) 321.
14. Suter, H. U., Huang, M.-B. and Engels, B. *J. Chem. Phys. 101* (1994) 7686.
15. Smith, G. R. and Weltner, W. *J. Chem. Phys. 62* (1975) 4592.
16. Danen, W. C. and Kensler, T. T. *J. Am. Chem. Soc. 92* (1970) 5235.
17. Danen, W. C. and Rickard, R. C. *J. Am. Chem. Soc. 94* (1972) 3254.
18. Hadley, S. G. and Volman, D. H. *J. Am. Chem. Soc. 89* (1967) 1053.
19. Qin, X.-Z. and Williams, F. *J. Phys. Chem. 90* (1986) 2292.
20. Sjöqvist, L., Lund, A., Eriksson, L. A., Lunell, S. and Shiotani, M. *J. Chem. Soc., Faraday Trans. 87* (1991) 1083.
21. Shiotani, M., Sjöqvist, L., Lund, A., Lunell, S., Eriksson, L. A. and Huang, M-B. *J. Phys. Chem. 94* (1990) 8081.
22. Bonazzola, L., Leray, N., Roncin, J. and Ellinger, Y. *J. Phys. Chem. 90* (1986) 5573.
23. Huang, M-B., Suter, H. U., Engels, B., Peyerimhoff, S. P. and Lunell, S. *J. Phys. Chem. 99* (1995) 9124.
24. Huang, M-B., Suter, H. U. and Engels, B. *Unpublished results.*
25. Huang, M-B., Suter, H. U. and Engels, B. *Chem. Phys. 183* (1993) 27.
26. Chipman, D. M. *Theor. Chim. Acta 76* (1989) 73.
27. Chipman, D. M. *J. Chem. Phys. 91* (1989) 5455.
28. Suter, H. U. and Engels, B. *Chem. Phys. Lett. In press.*
29. Engels, B., Perić, M., Reuter, W., Peyerimhoff, S. D. and Grein F. *J. Chem. Phys 97* (1992) 4996.
30. Engels, B. and Perić, M. *J. Chem. Phys. 96* (1992) 7629.

31. Perić, M. and Engels, B. *J. Chem. Phys. 97* (1992) 4996.
32. Staikova, M., Perić, M. and Engels, B. *J. Mol. Spectrosc. 163* (1994) 221.
33. Perić, M., Engels, B. and Peyerimhoff, S. D. In: Langhoff, S. R., Ed., *Understanding Chemical Reactivity*, Kluwer, Dordrecht, The Netherlands 1995, Vol. 13.
34. Perić, M., Engels, B. and Peyerimhoff, S. D. *J. Mol. Spectrosc. 150* (1991) 56.
35. Perić, M., Engels, B. and Peyerimhoff, S. D. *J. Mol. Spectrosc. 150* (1991) 70.
36. Perić, M., Engels, B. and Peyerimhoff, S. D. *J. Mol. Spectrosc. 174* (1995) 494.
37. Perić, M. and Engels, B. *J. Mol. Spectrosc. 174* (1995) 334.
38. Engels, B., Suter, H. U. and Perić, M. *J. Phys. Chem. 100* (1996) 10121.
39. Jungen, Ch. and Merer, A. J. In: Rao, K. N., Ed., *Molecular Spectroscopy: Modern Research*, Academic, New York, 1976, Vol. 2, p. 127.
40. Petelin, A. N. and Kiselev, A. A. *Int. J. Quantum Chem. 6* (1972) 701.
41. Perić, M., Peyerimhoff, S. D. and Buenker, R. J. *Mol. Phys. 55* (1985) 1129.
42. Knight, L. B. Jr., Kerr, K., Miller, P. K. and Arrington, C. A. *J. Phys. Chem. 99* (1995) 16842.
43. Ostojić, B., Perić, M. and Engels, B. *J. Mol. Spectrosc. Submitted for publication.*
44. Buenker, R. J. and Peyerimhoff, S. D. *Theor. Chim. Acta 35* (1974) 33.
45. Buenker, R. J. and Phillips, R. A. *J. Mol. Struct. (Theochem) 123* (1985) 291, and references cited therein.
46. Dunning, T. H., Jr. *J. Chem. Phys. 53* (1970) 2823.
47. Lie, G. C. and Clementi, E. *J. Chem. Phys. 60* (1974) 1275.
48. Thomas, J. T. Jr. and Andrews, L. *J. Am. Chem. Soc. 116* (1994) 4970.
49. Curtis, L. A. and Pople, J. A. *J. Chem. Phys. 91* (1989) 4809.

Received August 5, 1996.